Colloids and Surfaces B: Biointerfaces 103 (2013) 174–181

Contents lists available at SciVerse ScienceDirect

Colloids and Surfaces B: Biointerfaces

journal homepage: www.elsevier.com/locate/colsurfb

The characteristics and improved intestinal permeability of vancomycin PLGA-nanoparticles as colloidal drug delivery system

Parvin Zakeri-Milani[a], Badir Delf Loveymi[b,c], Mitra Jelvehgari[d], Hadi Valizadeh[e,*]

[a] Liver and Gastrointestinal Diseases Research Center and Faculty of Pharmacy, Tabriz University of Medical Sciences, Tabriz, Iran
[b] Biotechnology Research Center and Faculty of Pharmacy, Tabriz University of Medical Sciences, Tabriz, Iran
[c] Student Research Committee, Faculty of Pharmacy, Tabriz University of Medical Sciences, Tabriz, Iran
[d] Drug Applied Research Center and Faculty of Pharmacy, Tabriz University of Medical Sciences, Tabriz, Iran
[e] Research Center for Pharmaceutical Nanotechnology and Faculty of Pharmacy, Tabriz University of Medical Sciences, Tabriz, Iran

ARTICLE INFO

Article history:
Received 12 June 2012
Received in revised form 10 October 2012
Accepted 10 October 2012
Available online xxx

Keywords:
Vancomycin
Nanoparticles
PLGA
Intestinal permeability
SPIP

ABSTRACT

Aim: In the present investigation, vancomycin (VCM) biodegradable nanoparticles were developed for oral administration, with the aim of improving its intestinal permeability.
Methods: The vancomycin-loaded nanoparticles were prepared using double-emulsion solvent evaporation method. The prepared nanoparticles were characterized for their micromeritic and crystallographic properties, particle size, zeta potential, drug loading and release. Intestinal permeability of VCM nanoparticles was determined in different concentrations using SPIP technique in rats.
Results: Particle sizes were between 450 nm and 466 nm for different compositions of VCM-PLGA nanoparticles. Entrapment efficiency ranged between 38.38% and 78.6% with negative zeta (ζ) potential. The FT-IR, XRPD and DSC results ruled out any chemical interaction between the drug and PLGA. Effective intestinal permeability values of VCM nanoparticles in concentrations of 200, 300 and 400 μg/ml were significantly higher than that of solutions at the same concentrations.
Conclusion: Our findings suggest that PLGA nanoparticles could provide a delivery system for VCM, with enhanced intestinal permeability.

1. Introduction

Nanoparticulate polymeric delivery systems have been investigated as a possible approach to increase the oral drug availability. Biodegradable particulate carrier systems are of interest as potential means for oral delivery to enhance drug absorption, improve bioavailability and target therapeutic agents to particular organ [1–6]. Vancomycin (VCM) is a glycopeptide antibiotic used in the prophylaxis and treatment of serious, life-threatening infections caused by Gram-positive bacteria *e.g. Staphylococcus aureus* and other *Staphylococcus* species [7], that are unresponsive to other antibiotics [8,9]. It must be given intravenously (IV) for systemic therapy, since it is not absorbed from the intestine. It is a large hydrophilic molecule that partitions poorly across the gastrointestinal mucosa [10,11]. For oral macromolecular drug delivery, PLGA has been widely used. It is a commercially available, FDA-approved biodegradable polymer. The drug release can be controlled by the molecular weight of PLGA and the polymerization ratio of lactide to glycolide. Moreover, PLGA has proven to be safe because it decomposes to lactic acid and glycolic acid in the body and is finally excreted as CO_2 [3,12,13]. The degradation of these polyesters involves a bulk erosion process [14]. Since the bulk erosion can accelerate the diffusion and release of drug, the drug release mechanism based on these polyesters is quite complicated [12]. Both *in vitro* and *in vivo*, the PLGA co-polymer undergoes degradation in an aqueous medium through cleavage of its backbone ester linkages. This occurs by random hydrolytic chain scissions of the swollen polymer. However the role of enzymes in any PLGA biodegradation is unclear. Most of the literature indicates that the PLGA biodegradation does not involve any enzymatic activity and is purely through hydrolysis. However, some findings have suggested an enzymatic role in PLGA breakdown based on the difference in the *in vitro* and *in vivo* degradation rates [15]. Moreover polymer degradation can also be affected by the particle size. For instance, the rate of PLGA polymer degradation was found to increase with increasing particle size *in vitro* [16]. Polyesters provide alternative approaches to achieve desired release profiles and zero-order release kinetics due to their surface erosion mechanism [14]. Therefore, the ideal oral drug delivery

* Corresponding author at: Department of Pharmaceutics, Faculty of Pharmacy, Tabriz University of Medical Sciences, Tabriz, Iran. Tel.: +98 411 339 2649; fax: +98 411 334 4798.
E-mail addresses: valizadeh@tbzmed.ac.ir, valizadehh@gmail.com (H. Valizadeh).

0927-7765/$ – see front matter © 2012 Elsevier B.V. All rights reserved.
http://dx.doi.org/10.1016/j.colsurfb.2012.10.021

carrier should be biocompatible, small enough to pass through the gastrointestinal barrier, and should have an even size distribution without physical instability, such as aggregation. Indeed, a high drug encapsulation efficiency (EE %) is required to promote the pharmacological effects of a drug [14].

Loading of VCM, a hydrophilic antibiotic, into PLGA microparticles can be problematic owing to its high hydrophilicity. The most used technique to encapsulate hydrophilic molecules is double (water-in-oil-in-water, W/O/W) emulsification method, followed by solvent extraction/evaporation [17]. The encapsulation of VCM in PLGA microspheres has been described for the ocular delivery using emulsification/spray-drying in previous works [18]. Moreover, combination of VCM and VCM-loaded PLGA (75:25) microspheres blended with human grafts were evaluated *in vitro* for the intention of using for bone repair and to prevent infections [19]. However, there have been no reports on preparing VCM nanoparticles using PLGA and evaluating their intestinal permeability. It seems that alternative formulations are needed to extend the time over which the VCM intestinal level remains high enough and therefore enhance the oral performance of this antibiotic. Indeed, the presence of a polymeric wall provides protection from the gastrointestinal environment and may favor prolonged contact with the epithelium that may be sufficient to increase the bioavailability of certain drugs. On the other hand, intestinal permeability of a drug is an important and determining factor for its oral bioavailability. One of the most used classic techniques in the study of intestinal absorption of compounds has been the single-pass intestinal perfusion (SPIP) model [20–24], which provides experimental conditions closer to what is faced following oral administration. This technique has lower sensitivity to pH variations because of a preserved microclimate above the epithelial cells and it maintains an intact blood supply to the intestine [20–24]. Since human *in vivo* studies are not usually possible in the early phases of drug development, some experimental methods such as animal *in vivo* and *ex vivo* models have so far been evolved to estimate gastrointestinal absorption of drugs [20,23]. The goal of this study was to investigate the entrapment of VCM into PLGA nanoparticles, with the aim of improving its intestinal permeation.

2. Materials and methods

2.1. Materials

Vancomycin hydrochloride was obtained from Jaberebnehyan Pharmaceutical Company, Iran. Poly (D,L-lactide-co-glycolide) (PLGA) (50:50 D,L-lactide:glycolide) with average molecular weight of 12,000 g/mol (Resomer RG 502), was purchased from Boehringer Ingelheim, Germany. Poly vinyl alcohol (PVA) with a molecular weight of 95,000 D (Acros Organics, Geel, Belgium) and dichloromethane, methanol, glacial acetic acid, triethanolamine, hydrochloric acid, potassium chloride, sodium chloride, sodium hydrogen phosphate and potassium dihydrogen phosphate all were obtained from Merck (Darmstadt, Germany). Silastic membrane (# 10,000 Da) was provided by Biogene (Mashhad, Iran). Male Wistar rats were purchased from the animal house of Tabriz University of Medical Sciences. In all animal studies, The Guide to the Care and Use of Experimental Animals by the Canadian Council on Animal care was followed.

2.2. Preparation of nanoparticles

VCM-loaded PLGA nanoparticles were prepared by the $W_1/O/W_2$ modified solvent evaporation method using different ratios of drug to polymer (1:0.5, 1:1 and 1:2). Briefly, 5 ml of aqueous internal phase (containing 50 mg VCM) was emulsified for 15 s in 20 ml of methylene chloride (containing 25, 50 and 100 mg PLGA) using a homogenizer with 22,000 rpm. This primary emulsion was poured into 25 ml of a 0.2% PVA aqueous solution while stirring in a homogenizer for 3 min and immersed in an ice water bath to create the water in an oil-in-water emulsion. 3–4 ml of nanoparticle suspension was obtained after solvent evaporation under reduced pressure (Evaporator, Heidolph, USA). Nanoparticles were separated from the bulk suspension by centrifugation (Hettich Universal 320R, USA) at 22,000 × *g* for 20 min. The supernatant was kept for drug assay as described later. Nanoparticles were collected by filtration and washed with three portions of 30 ml of water and redispersed in 3 ml of purified water before freeze-drying. The freeze-dried nanoparticles were re-suspended in 2 ml of purified water shortly before permeability and other studies. Blank nanoparticles were prepared under the same conditions without drug [25,26].

2.3. Nanoparticle size and zeta potential measurement

A laser light scattering particle size analyzer (SALD-2101, Shimadzu, Japan) was used to determine the particle size of the drug, polymer and nanoparticles. Samples were suspended in distilled water (nanoparticles and polymer) or acetone (drug) in a 1 cm cuvette and stirred continuously during the particle size analysis. Zeta potential, which is electric potential in the interfacial double layer at the location of the slipping plane *versus* a point in the bulk fluid away from the interface [27], was measured by Zetasizer (Malvern instruments, England). VCM nanoparticles were diluted with deionized water before measurement. Each measurement was carried out in triplicate.

2.4. Determination of drug loading and loading efficiency

The loading efficiency of VCM in PLGA nanoparticles was determined spectrophotometrically (UV-160, Shimadzu, Japan) at 280.2 nm by measuring the amount of non-entrapped VCM in the external aqueous solution (indirect method) before freeze-drying. In the case of nanoparticles, the external aqueous solution was obtained after centrifugation of the colloidal suspension for 20 min at 22,000 × *g*. A standard calibration curve was plotted with the VCM solution (aqueous solution of 0.2% PVA). The loading efficiency (%) was calculated according to the following equation [28]:

$$\text{Loading efficiency}\,(\%) = \left(\frac{\text{actual drug content in nanoparticles}}{\text{theoretical drug content}}\right) \times 100$$

The production yield of the nanoparticles was determined by calculating accurately the initial weight of the raw materials and the last weight of the polymeric particles obtained. All of the experiments were performed in triplicate.

2.5. Infrared spectroscopy, differential scanning calorimetry (DSC) and X-ray diffraction studies

The infrared (IR) spectra of VCM powder, physical mixture of drug and polymer, and prepared nanoparticles were recorded on an IR-spectrophotometer (Bomem Hartmann & Brann, Canada) by the KBr pellet technique. Differential scanning calorimetry (DSC) analysis was performed using a DSC-60 calorimeter (Shimadzu, Japan). The instrument was equipped with a TA-60WS thermal analyzer, FC-60A flow controller and TA-60 software. Samples of VCM, physical mixture and agglomerates were sealed in an aluminum crucible and heated at a rate of 10 °C min^{-1} up to 300 °C under a nitrogen atmosphere. A similar empty pan was used as

reference. Powder X-ray diffraction patterns (XRD) of the pure drug and spherical agglomerates were obtained using an X-ray diffractometer (Siemens D5000, Munich, Germany) equipped with a graphite crystal monochromator (CuKα) (a voltage of 40 KV and a current of 20 mA) radiations to observe the physical state of the drug in the microspheres. The scanning rate was 6°/min over the range of 5–70° with an interval of 0.02°.

2.6. Dissolution study

VCM dissolution patterns from freeze-dried nanoparticles were evaluated under sink conditions. Dissolution studies were carried out using a dialysis membrane rotating method for all nanoparticle formulations. A set amount of nanoparticles (equivalent to 100 mg drug) was added to 200 ml dissolution medium (saline phosphate buffer, pH 7.4), preheated and maintained at 37 ± 1 °C in a water bath, and stirred at 100 rpm. Then 1 ml of suspension was withdrawn at appropriate time intervals (0.5, 1, 2, 3, 4, 5, 6, 8, 12 and 24 h) and centrifuged at 22,000 × *g* for 10 min. The filtrate was replaced by 3 ml of fresh buffer. The amount of VCM in the release medium was determined by UV at 279.8 nm [26].

2.7. Perfusion solution

The perfusion solution was prepared by dissolving 7 g NaCl, 0.2 g KCl, 1.44 g Na_2HPO_4 and 0.24 g KH_2PO_4 in one liter of distilled water. The pH of prepared phosphate buffered saline was 7.4. Preliminary experiments showed that there was no considerable adsorption of the compounds on the tubing and syringe [23].

2.8. In situ permeation studies

Adult male Wistar rats (200–250 g) were obtained from the Animal Center of the local University, Tabriz, Iran. They were housed in air conditioned quarters under a photoperiod schedule of 12 h light/12 h dark. They received standard laboratory diet and tap water, available *ad libitum*. Rats were divided into control and test groups. In each group three concentration levels of VCM (200, 300 and 400 μg/ml) were used in separate experiments. The anaesthetized rats were restrained in a supine position on a board kept at 37 °C. A small midline incision was made in the abdomen and a 10 cm section of the small intestine was identified and cannulated. Blank perfusion buffer was infused for 10 min by a syringe pump (Palmer, England) followed by perfusion of different concentrations (200, 300, 400 μg/ml) of VCM (prepared from its powder or its nanoparticles) at a flow rate of 0.2 ml/min for 90 min. Outlet samples were collected at appropriate intervals (30, 40, 50, 60, 70, 80 min) in microtubes. The volume of sample for each time interval was 2 ml. When the experiment was completed, the length of segment was measured and the animal was euthanatized with a cardiac injection of saturated solution of sodium pentobarbital. Samples were stored at −20 °C until analysis. Samples from perfusion study were filtered and directly injected onto HPLC column and required no sample preparation prior to analysis. Effective permeability coefficients (P_{eff}) were calculated from the steady-state concentrations of compounds in the collected perfusate, which is considered to be reached when the concentration level of phenol red was at the steady state level. It was reached about 40 min after the beginning of the perfusion, which is confirmed by plotting the ratio of the outlet to inlet concentrations (corrected for water transport) *versus* time. The intestinal net water flux (NWF, μl/h/cm) was calculated according to following equation:

$$\mathrm{NWF} = Q_{in}\frac{1-(\mathrm{Ph.red}_{out}/\mathrm{Ph.red}_{in})}{1}$$

where [Ph.red $_{(in)}$] and [Ph.red $_{(out)}$] are the inlet and outlet concentrations of the non-absorbable water flux marker phenol red. A negative net water flux indicates loss of fluid from the mucosal side (lumen) to the serosal side (blood). A positive net water flux indicates secretion of fluid into the segment [29]. P_{eff} was calculated using the following equation according to the parallel tube model:

$$P_{eff} = -Q\ \ln\frac{C_{out}/C_{in}}{2\pi rl}$$

In which C_{in} is the inlet concentration and C_{out} is the outlet concentration of compound which is corrected for volume change in segment using phenol red concentration in inlet and outlet tubing. Q is the flow rate (0.2 ml/min), r is the rat intestinal radius (0.18 cm) and l is the length of the segment.

2.9. Chromatographic conditions

Perfusion samples were analyzed using a modified reversed-phase high performance liquid chromatography (RP-HPLC) method. The analytical procedure was validated for specificity, accuracy, precision and sensitivity. A liquid chromatographic system (Knauer, Germany) comprised of Knauer K1000 solvent delivery module equipped with a Rheodyne (Cotati, CA) injector and a variable wavelength ultraviolet spectrophotometric detector (Knauer smartline 2500) set at 430 nm and 254 nm for phenol red and VCM, respectively. EZChrom Elite version 2.1.7 was used for data acquisition, data reporting and analysis. The mobile phase for VCM analysis consisted of 30% (v/v) methanol and 70% (v/v) of glacial acetic acid aqueous solution (0.75%) adjusted to pH 5.5. Analytical column used for chromatographic separations was C18 (250 mm × 4.6 mm) 5 μm with precolumn. For phenol red analysis the mobile phase consisted of 45% (v/v) KH_2PO_4 0.05 M and 55% (v/v) methanol adjusted to pH 2.6. Under the mentioned conditions the retention times for VCM and phenol red were 5 min and 13.8 min, respectively. Runs contained quality control samples (QC) at three concentrations levels. Calibration curves were obtained by plotting the phenol red and VCM peak area against their concentrations in standard solutions [20].

3. Results

3.1. Micromeritics properties

Encapsulation efficiencies, mean particle diameter and production yield of the different VCM nanoparticles are reported in Table 1. It is evident from Table 1 that the encapsulation efficiency was affected by the ratio of drug:polymer. The particle size data show that prepared nanoparticles were of submicron size and of low polydispersity, which indicated a relatively narrow particle size distribution. An increase in particle size from 450 nm to 466 nm with a decrease in the theoretical drug loading was also observed (Table 1). It has also been reported that the particle size increases with increasing the content in polymer. A volume-based size distribution indicated a log–probability distribution. The increase in drug content of the nanoparticles with increased theoretical drug loading has resulted in decreased particle size ($p < 0.05$). In this case, the viscosity of the inner phase of the polymer did not seem to have a great influence on the particle diameter. The average yield of 96% is in the normal range and does not indicate any unexpected loss of products. The results showed that this led to a corresponding increase in polymer content from 0.33% to 0.66% (w/w); however the corresponding drug entrapment decreased from 48.8% to 12.8%. The zeta potential measurements showed small negatively charged particle surfaces, varying from −6.7 mV to −10.9 mV (Table 1). All the obtained values were then acceptable and favoring a good stability.

Table 1
Effect of drug: polymer ratio on drug loading efficiency, production yield, particle size zeta potential and polydispersity index of vancomycin nanoparticles.

Formulation	Drug:polymer ratio	Production yield (% ± SD)	Theoretical drug content (%)	Mean drug entrapped (% ± SD)	Drug loading efficiency ± SD) %)	Mean particle size (nm ± SD)	Zeta potential (mV ± SD)	Polydispersity index (PDI)
F_1	1:0.5	95 ± 1.52	66.67	44.80 ± 0.98	78.6 ± 2.38	450 ± 35.29	−7.28 ± 7.58	0.006
F_2	1:1	96 ± 1.15	50	33.58 ± 1.48	67.1 ± 2.46	461 ± 33.45	−7.07 ± 5.96	0.0053
F_3	1:2	97 ± 1.02	33.33	12.77 ± 1.18	38.38 ± 2.25	466 ± 38.80	−3.57 ± 7.21	0.0069

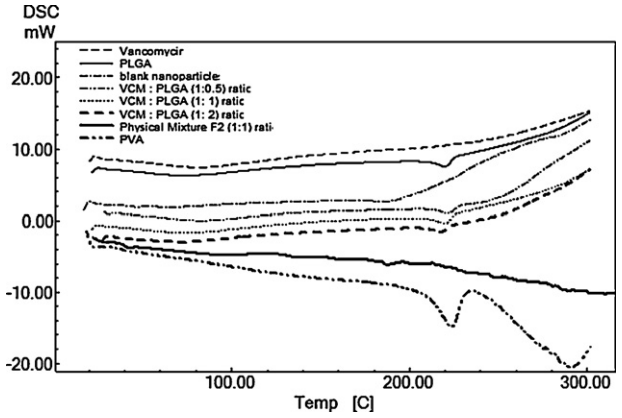

Fig. 1. DSC thermogram of the VCM; PLGA; PVA; physical mixture F_2; blank nanoparticles, VCM nanoparticles formulations as F_1, F_2 and F_3.

3.2. DSC analysis

The DSC thermogram of VCM and the polymer had no endotherms, demonstrating their amorphous state (Fig. 1). The physical mixture of VCM and PLGA showed nearly the same thermal behavior as the individual components, indicating that there was no interaction between the drug and the polymer in the solid state. In the thermogram of the PLGA-based nanoparticles there was a small endothermic peak at 220–222 °C which corresponds to the phase transition of PVA (Fig. 1). Based on thermodynamic calculations on the enthalpy of this endotherm, considering the heat flow of PVA in nanoparticles (52.97, 55.26 and 28.40 mJ for F_1, F_2 and F_3 formulations respectively), the estimated loading of PVA in F_1, F_2 and F_3 formulations was calculated to be 12.74%, 13.29% and 6.83%, respectively.

3.3. Powder X-ray diffractometry

Comparison of the X-ray diffraction patterns of VCM (Fig. 2a) and its nanoparticles prepared with PLGA (Fig. 2e–g) showed no significant change in the peak intensities, suggesting that the amorphous nature of VCM was not affected by the polymer.

3.4. FTIR studies

The Fourier transform IR spectrum of VCM showed phenolic OH at 3257.39 cm^{-1}, aromatic C=C stretching at 1652.7 cm^{-1} and C=O stretching at 1503.48 cm^{-1}. The FTIR spectra of VCM-loaded PLGA nanoparticles, physical mixture F_2 (1:1), and the individual components are depicted in Fig. 3. The amide I (1600–1700 cm^{-1}) and amide II (1500–1600 cm^{-1}) regions of PLGA are depicted in Fig. 3b. For nanoparticles F_1, F_2 and F_3, C=O stretching bands are seen at 1675.1, 1751, 1752.1 cm^{-1}, respectively (Fig. 3e–g) [30]. No differences in the positions of the absorption bands of VCM were observed in spectra of the prepared formulations, indicating that there are no chemical interactions in the solid state between the drug and the polymer.

3.5. In vitro release study

The mean cumulative release percent *versus* time curves are shown in Fig. 4. The rate of dissolution of physical mixture was

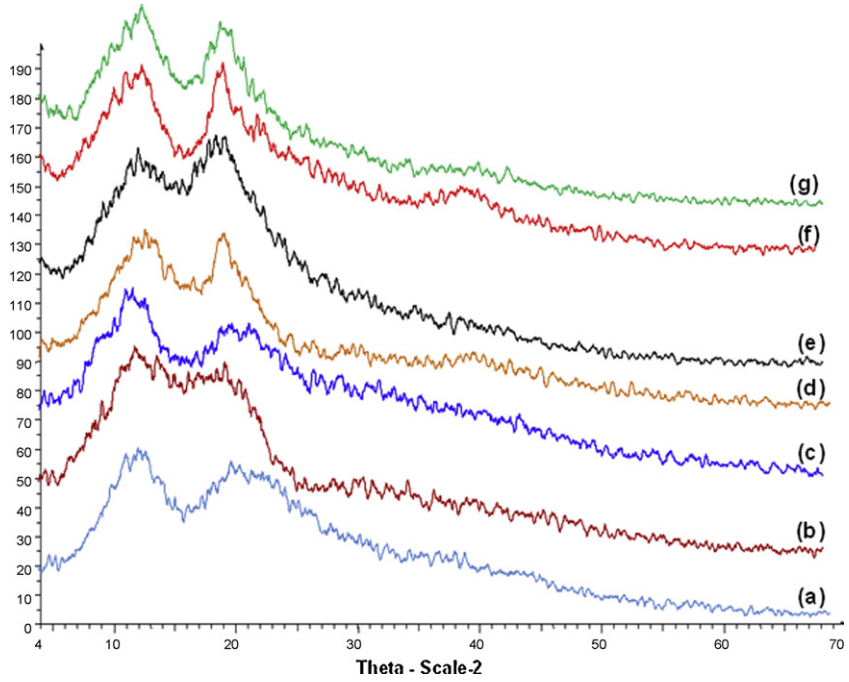

Fig. 2. X-ray diffraction patterns of: (a) VCM; (b) PLGA; (c) physical mixture F_2; (d) blank nanoparticles; (e) VCM:PLGA (1:0.5); (f) VCM:PLGA (1:1); (g) VCM:PLGA (1:2).

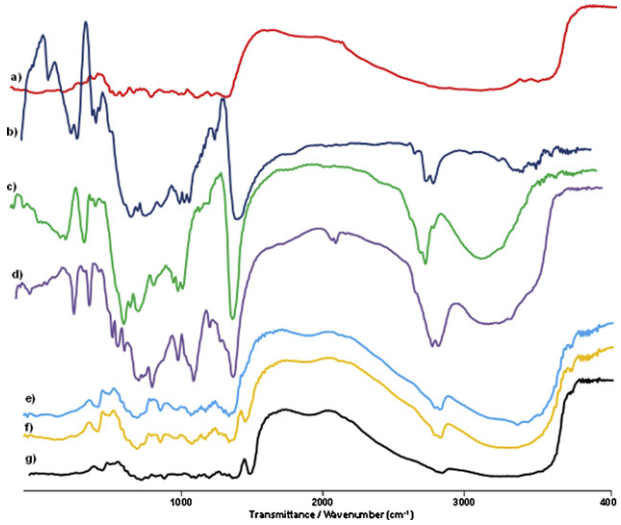

Fig. 3. FTIR spectrum: (a) PLGA; (b) VCM; (c) physical mixture F_2; (d) blank nanoparticles; (e) VCM:PLGA (1:0.5); (f) VCM:PLGA (1:1); (g) VCM:PLGA (1:2).

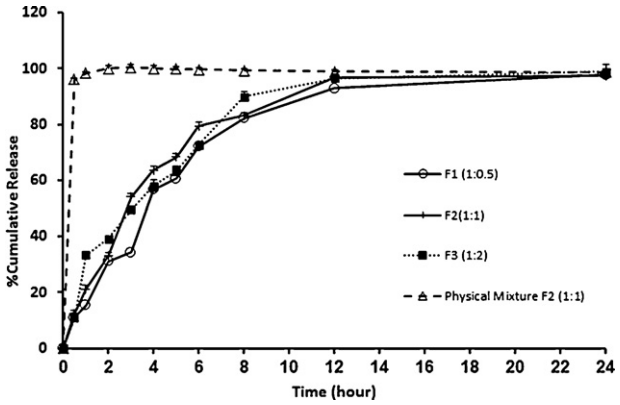

Fig. 4. Cumulative percent release of VCM nanoparticles prepared with different drug-to-polymer ratio and physical mixture F_2. (Δ) Physical mixture (1:1); (○) 1:0.5 nanoparticles; (+) 1:1 nanoparticles; (■) 1:2 nanoparticles. Symbols represent the mean ± SD at each time point ($n = 3$).

quite fast, and more than 96% drug was dissolved in about 30 min (Table 2, Fig. 4). The drug release from the nanoparticles appeared to have two components with a burst release of about 10.78–12.27% at the first sampling time of 30 min. This was followed by a slower exponential release of the remaining drug over the next 6–8 h. It is speculated that a reduced diffusion path and increased tortuosity may have retarded the drug release from the matrix in the presence of polymer matrix. Furthermore, Fig. 4 clearly illustrates that the rate of drug release from nanoparticles is independent on the polymer content of nanoparticles and all preparations exhibited similar dissolution efficiencies ($p > 0.05$). As shown in Table 2, the lowest dissolution efficiency was observed for F_1 (77.97%) while the dissolution efficiency of the physical mixture was 98.13% ($p < 0.05$). The value of $t_{50\%}$ varied between 2.84 (F_3 formulation) to 3.73 h (F_3 formulation). The calculated difference factor (f_1) [31–36] showed that there was no similarity between the release profiles of nanoparticle formulations and physical mixture (Table 2). In order to find out the mechanism of drug release, the *in vitro* release profiles were fitted to various kinetic models (Higuchi, first-order, Peppas and zero-order) [36–43]. Dissolution rate constants were calculated from the slope of the respective plots. High correlation was observed for the first order and Peppas models (Table 2).

3.6. Intestinal permeability data

In any *in situ* intestinal perfusion technique it is necessary to determine the extent of volume changes of the solution in the gut lumen during an experiment. For this purpose phenol red dye (200 μg/ml) was added to drug solution in each experiment. Phenol red was used as a non-absorbable marker to detect gain or loss of water by the lumen. The determined mean P_{eff} values for different concentrations of vancomycin and its nanoparticles in PBS and also

Table 2
Comparison of various release characteristics of vancomycin from different nanoparticle formulations and physical mixture together with their release kinetic fitting parameters.

	Release parameter	F_1	F_2	F_3	Physical mixture
	[a] $t_{50\%}$ (h)	2.98	3.73	2.84	0.26
	[b] DE	77.97	78.48	82.19	98.13
	[c] $Q_{0.5}$	11.11 ± 0.76	12.27 ± 1.25	10.78 ± 1.25	96.07 ± 0.51
	[d] Q_{24}	97.71 ± 0.75	97.36 ± 1.02	98.96 ± 2.53	98.70 ± 0.62
	[e] f_1 value	39.79	44.11	38.47	0.22
Zero order $f = kt$	K_0	0.0405	0.03839	0.0383	0.0131
	RSQ	0.6869	0.6147	0.6473	0.0932
	MPE %	2384988.55	2954566.272	2986174.829	7463490.366
First order $\mathrm{Ln}(1-f) = kt$	K_1	−0.1669	−0.1671	−0.2019	−0.1933
	RSQ	0.9594	0.8687	0.9471	0.5264
	MPE %	1033119.669	2273243.928	1386058.494	8784441.933
Peppas model $\mathrm{Ln}f = \ln k + b\ln t$	b	0.48	0.45	0.42	0.0070
	k_p	0.2374	5.2337	0.2298	0.1156
	RSQ	0.9009	0.8697	0.8919	0.2784
	MPE %	22.6480	23.83227	19.3823	11.4406
Higuchi model $f = kt^{0.5}$	K_h	1.6236	1.5631	1.5194	1.0070
	RSQ	0.5567	0.5671	50.5426	0.4922
	MPE %	4420383.624	6265335.71	5526267.873	98114353.76

[a] Dissolution time for 50% fractions.
[b] Dissolution efficiency.
[c] Amount of drug release after 0.5 h.
[d] Amount of drug release after 24 h.
[e] Difference factor [32,36].

Table 3
Permeability coefficients determined in rats for test and control groups.

Group	C_{in}	Mean P_{eff} ($\times 10^5$ cm/s)	Mean NWF (ml/min/cm)
Control	200	6.11(±2.66)	0.0001(±0.0006)
	300	3.87(±2.45)	0.0004(±0.0004)
	400	2.54 (±1.64)	0.0000(±0.0003)
Test	200	17.88 (±2.61)	0.0007(±0.0004)
	300	16.63(±2.98)	0.0006(±0.0007)
	400	15.75(±4.47)	−0.0001(±0.0004)

the mean net water fluxes in the single pass intestinal perfusion technique are listed in Table 3.

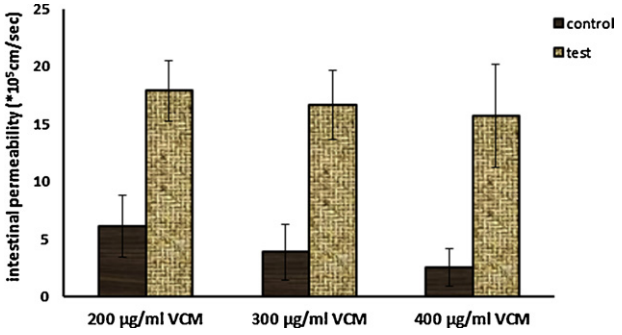

Fig. 5. Intestinal permeability of VCM from prepared nanoparticles with different drug concentrations. Symbols represent the mean ± SD ($n = 4$).

4. Discussion

The organic phase (O) acts as a barrier between the two aqueous compartments. To control the methylene chloride removal time and rate, we used a rotary evaporator method. Thus, the migration of the drug into the external phase (W_2) was impeded. The particle formation itself is based on coacervation. In general, the solvent removal rate directly affects the encapsulation efficiency of the drug [14,44]. Slow membrane formation rate may reduce the encapsulation efficiency as a result of enhancing the chances of drug molecules to be diffused out from the inner W_1 phase to outer W_2 water phase through the water channels of the PLGA membrane before perfect hardening of the PLGA membrane [14,45,46]. Therefore, rapid membrane formation is an important criterion preventing the leakage of VCM to the outer W_2 water phase. Generally, PVA is used as a dispersing agent in the $W_1/O/W_2$ emulsion method. It lowers the surface tension between the PLGA surface and the W_2 water phase [14,47]. However, because PVA cannot be washed away perfectly, it remains on the surface of PLGA [14,48]. PVA concentration in the external water phase is known to be a key factor to influence the size of nanoparticles [14]. The low drug incorporation efficiency may be attributed to the water soluble nature of VCM hydrochloride. This led to its rapid partitioning into the aqueous phase and hence decreased entrapment into the nanoparticles during polymer deposition. The decreased drug entrapment with increasing theoretical drug loadings is due to an enhanced drug leakage into the aqueous phase at high loadings. All formulations showed negative zeta potential (Table 1), which promotes particle stability, as the repulsive forces prevent aggregation with aging [49]. It has been reported that the negative charge of PLGA nanoparticles is due to the ionization of carboxylic groups of surface polymer [49,50]. An increase in theoretical drug loadings led to a slight decrease in Zeta potential from −7.58 mV to −3.5 mV. These findings are in accordance with what was expected, a decrease in the surface negativity due to interaction of carboxyl groups and the cationic drug on the particle surface. Zeta potential is also an important factor to determine particles interaction *in vivo* with the cell membrane. In biological systems, for example, the zeta potential gives clues to how cells are interacting and whether pharmacologically active agents, for instance, are binding to their targets properly [51].

The increase in nanoparticle size with increases in the theoretical drug loading of VCM (Table 1) may possibly have influenced the surface charge of the PLGA nanoparticles [52]. The results of this study, however, agree with those of Chasteigner and coworkers [53] who reported a decrease in the negative surface charge when itraconazole was loaded into polycaprolactone nanoparticles. From the data it is evident that all the formulations are almost unstable in the colloidal state. This suggests that the particles should not be stored in a liquid suspension form and rather they should be stored in a lyophilized state [52]. The rapid initial release of VCM was probably due to the drug which was adsorbed at or close to the surface of the nanoparticles and the large surface to volume ratio of nanoparticle geometry because of their size [50]. It may also be due to the water soluble nature of VCM. The exponential delayed release may be attributed to diffusion of the dissolved drug within the PLGA core of the nanoparticle into the dissolution medium. Similar observations were reported by other researchers working on paclitaxel and enalapril-PLGA nanoparticles [54,55]. Loading of VCM into the nanoparticles leads to a modulation of *in vitro* drug release, depending on their composition. The data obtained were also put in Korsemeyer-Peppas model in order to find out the n value, which describes the drug release mechanism. The n value of microspheres of different drug:polymer ratio was between 0.42 and 0.48, indicating that the drug release was diffusion controlled (Table 2).

On the other hand, the obtained results in rats demonstrates that the intestinal permeability of VCM is significantly increased using its nanoparticles in all three concentrations ($p < 0.05$). The stable water fluxes and permeability coefficients in each perfusion, as a function of time, for tested compounds indicated that intestinal barrier function was maintained during the procedure. The intestinal permeability of VCM solution was determined to be in the range of 2.54 (±1.64) × 10^{-5} cm/s–6.11 (±2.66) × 10^{-5} cm/s in control groups. However, the drug permeability in test groups' intestinal segments which were perfused by VCM nanoparticles in PBS, ranged between 15.75 (±4.47) × 10^{-5} cm/s and 17.88 (±2.61) × 10^{-5} cm/s. Although a significant enhancement of VCM effective permeability was reached in all three concentration levels in test groups (Fig. 5), there were no statistical differences among the P_{eff} values for different concentrations. Therefore, it seems that the intestinal permeability of VCM is not concentration-dependent. Considering the hydrophilicity and high molecular weight of the VCM, the higher intestinal permeability of VCM nanoparticles is likely due to large specific surface area and enhanced paracellular passage and endocytotic uptake, because particles of less than 500 nm in diameter are absorbed by intestinal enterocytes through endocytosis. The similar results were reported by Kaili et al. for docetaxel. Docetaxel nanoparticles with particle size under 500 nm had efficient uptake in the intestine, particularly in the lymphoid sections, where they could bypass the liver first-pass metabolism. Moreover the sustained-release characteristic of the nanoparticles increased the circulation time of docetaxel, which prolonged the drug residence time in systematic circulation and resulted in better bioavailability. The absolute bioavailability of docetaxel nanoparticles was 3.65 times that of docetaxel solution [56]. The size-dependent absorption of polymeric nanoparticles was also reported by He et al. for protein drugs [57]. In the present study coating of VCM nanoparticles with PVA, a bioadhesive material, can also be a strategy to increase nanoparticle uptake by intestinal enterocytes. Nanoparticles coated with bioadhesive materials are used to obtain mucoadhesive properties. Adhesion of a carrier system to the mucus may improve residence time and drug

contact with the underlying epithelium, thus increasing intestinal permeability.

5. Conclusion

VCM-loaded poly (lactide-co-glycolide) (PLGA) nanoparticles were successfully prepared by using $W_1/O/W_2$ double-emulsion solvent evaporation method. Drug release from nanoparticles was more sustained than physical mixture. Moreover, the intestinal permeation of VCM was improved using its nanoparticles and this may allow more efficient therapy compared to VCM formulations present in the market.

Declaration of interest

The authors report no conflicts of interest. The authors alone are responsible for the content and writing of the paper.

Acknowledgments

The financial support from Liver and Gastrointestinal Diseases Research Center, and Research Center for Pharmaceutical Nanotechnology, Tabriz University of Medical Sciences is greatly acknowledged.

References

[1] M.P. Desai, V. Labhasetwar, G.L. Amidon, R.J. Levy, Gastrointestinal uptake of biodegradable microparticles: effect of particle size, Pharm. Res. 13 (1996) 1838.
[2] L. Yu, L. Zhou, M. Ding, J. Li, H. Tan, Q. Fu, X. He, Synthesis and characterization of novel biodegradable folate conjugated polyurethanes, J. Colloid Interface Sci. 358 (2011) 376.
[3] M.M. Yallapu, B.K. Gupta, M. Jaggi, S.C. Chauhan, Fabrication of curcumin encapsulated PLGA nanoparticles for improved therapeutic effects in metastatic cancer cells, J. Colloid Interface Sci. 351 (2010) 19.
[4] G.S. Kumar, E.K. Girija, A. Thamizhavel, Y. Yokogawa, S.N. Kalkura, Synthesis and characterization of bioactive hydroxyapatite–calcite nanocomposite for biomedical applications, J. Colloid Interface Sci. 349 (2010) 56.
[5] C. Nouvel, J. Raynaud, E. Marie, E. Dellacherie, J.L. Six, A. Durand, Biodegradable nanoparticles made from polylactide-grafted dextran copolymers, J. Colloid Interface Sci. 330 (2009) 337.
[6] S. Hallaj-Nezhadi, H. Valizadeh, S. Dastmalchi, B. Baradaran, M.B. Jalali, F. Dobakhti, F. Lotfipour, Preparation of chitosan-plasmid DNA nanoparticles encoding interleukin-12 and their expression in CT-26 colon carcinoma cells, J. Pharm. Pharm. Sci. 14 (2011) 181.
[7] J.T. DiPiro, R.L. Talbert, G.C. Yee, G.R. Matzke, B.G. Wells, L.M. Posey, Pharmacotherapy, MCGRAW-HILL Medical Publishing Division, New York, 2005.
[8] D.P. Han, S.R. Wisniewski, L.A. Wilson, M. Barza, A.K. Vine, B.H. Doft, S.F. Kelsey, Spectrum and susceptibilities of microbiologic isolates in the endophthalmitis vitrectomy study, Am. J. Ophthalmol. 122 (1996) 1.
[9] H. Okochi, M. Nakano, Preparation and evaluation of w/o/w type emulsions containing vancomycin, Adv. Drug Deliv. Rev. 45 (2000) 5.
[10] J.M. Pogue, D.D. DePestel, D.R. Kaul, Y. Khaled, D.G. Frame, Systemic absorption of oral vancomycin in a peripheral blood stem cell transplant patient with severe graft-versus-host disease of the gastrointestinal tract, Transpl. Infect. Dis. 11 (2009) 467.
[11] S. Rao, Y. Kupfer, M. Pagala, E. Chapnick, S. Tessler, Systemic absorption of oral vancomycin in patients with *Clostridium difficile* infection, Scand. J. Infect. Dis. 43 (2011) 386.
[12] C. Damge, H. Vranckx, P. Balschmidt, P. Couvreur, Poly(alkyl cyanoacrylate) nanospheres for oral administration of insulin, J. Pharm. Sci. 86 (1997) 1403.
[13] G. Mohammadi, H. Valizadeh, M. Barzegar-Jalali, F. Lotfipour, K. Adibkia, M. Milani, M. Azhdarzadeh, F. Kiafar, A. Nokhodchi, Development of azithromycin-PLGA nanoparticles: physicochemical characterization and antibacterial effect against *Salmonella typhi*, Colloids Surf. B 80 (2010) 34.
[14] Y.-Y. Yang, T.-S. Chung, N. Ping Ng, Morphology, drug distribution, and in vitro release profiles of biodegradable polymeric microspheres containing protein fabricated by double-emulsion solvent extraction/evaporation method, Biomaterials 22 (2001) 231.
[15] M.S. Muthu, Nanoparticles based on PLGA and its co-polymer: an overview, Asian J. Pharm. 3 (2009) 266.
[16] M. Dunne, I. Corrigan, Z. Ramtoola, Influence of particle size and dissolution conditions on the degradation properties of polylactide-co-glycolide particles, Biomaterials 21 (2000) 1659.
[17] W. Hachicha, L. Kodjikian, H. Fessi, Preparation of vancomycin microparticles: importance of preparation parameters, Int. J. Pharm. 324 (2006) 176.
[18] E. Gavini, P. Chetoni, M. Cossu, M.G. Alvarez, M.F. Saettone, P. Giunchedi, PLGA microspheres for the ocular delivery of a peptide drug, vancomycin using emulsification/spray-drying as the preparation method: in vitro/in vivo studies, Eur. J. Pharm. Biopharm. 57 (2004) 207.
[19] B. Sayin, B. Atilla, S. Çaliş, S. Marangoz, A.A. Hincal, In vivo evaluation of intraarticular vancomycin delivery following implantation of antibiotic loaded allografts and biopolymeric microparticules into bone defects, in: XXIII SICOT/SIROT Triennial World Congress, Istanbul-Turkey, 2005.
[20] H. Valizadeh, P. Zakeri-Milani, Z. Islambulchilar, H. Tajerzadeh, A simple and rapid high-performance liquid chromatography method for determining furosemide, hydrochlorothiazide, and phenol red: applicability to intestinal permeability studies, J. AOAC Int. 89 (2006) 88.
[21] P. Zakeri-Milani, M. Barzegar-Jalali, M. Azimi, H. Valizadeh, Biopharmaceutical classification of drugs using intrinsic dissolution rate (IDR) and rat intestinal permeability, Eur. J. Pharm. Biopharm. 73 (2009) 102.
[22] P. Zakeri-Milani, H. Valizadeh, Z. Islambulchilar, S. Damani, M. Mehtari, Investigation of the intestinal permeability of ciclosporin using the in situ technique in rats and the relevance of P-glycoprotein, Arzneimittelforschung 58 (2008) 188.
[23] P. Zakeri-Milani, H. Valizadeh, H. Tajerzadeh, Y. Azarmi, Z. Islambolchilar, S. Barzegar, M. Barzegar-Jalali, Predicting human intestinal permeability using single-pass intestinal perfusion in rat, J. Pharm. Pharm. Sci. 10 (2007) 368.
[24] P. Zakeri-Milani, H. Valizadeh, H. Tajerzadeh, Z. Islambulchilar, The utility of rat jejunal permeability for biopharmaceutics classification system, Drug Dev. Ind. Pharm. 35 (2009) 1496.
[25] A.S. Hasan, M. Socha, A. Lamprecht, F.E. Ghazouani, A. Sapin, M. Hoffman, P. Maincent, N. Ubrich, Effect of the microencapsulation of nanoparticles on the reduction of burst release, Int. J. Pharm. 344 (2007) 53.
[26] V. Hoffart, N. Ubrich, C. Simonin, V. Babak, C. Vigneron, M. Hoffman, T. Lecompte, P. Maincent, Low molecular weight heparin-loaded polymeric nanoparticles: formulation, characterization, and release characteristics, Drug Dev. Ind. Pharm. 28 (2002) 1091.
[27] Zeta potential of colloids in water and waste water, in: ASTM Standard D 4187-82, American Society for Testing and Materials, West Conshohocken, PA, USA, 1985.
[28] M. Jelvehgari, P. Zakeri-Milani, M.R. Siahi-Shadbad, B.D. Loveymi, A. Nokhodchi, Z. Azari, H. Valizadeh, Development of pH-sensitive insulin nanoparticles using Eudragit L100-55 and chitosan with different molecular weights, AAPS PharmSciTech 11 (2010) 1237.
[29] U. Fagerholm, M. Johansson, H. Lennernas, Comparison between permeability coefficients in rat and human jejunum, Pharm. Res. 13 (1996) 1336.
[30] S.K. Sahoo, A.A. Mallick, B. Barik, P.C. Senapat, Formulation and in vitro evaluation of eudragit® microspheres of stavudine, Trop. J. Pharm. Res. 4 (2005) 369.
[31] United States Pharmacopoeia and National Formulary (USP 31-NF26), Rockville, MD, 2008.
[32] J.W. Moore, H.H. Flanner, Mathematical comparison of curves with an emphasis on in vitro dissolution profiles, Pharm. Tech. 20 (1996) 64.
[33] S.M. Alli, Preparation and characterization of a coacervate extended-release microparticulate delivery system for *Lactobacillus rhamnosus*, Int. J. Nanomedicine 6 (2011) 1699.
[34] S.M. Alli, S.M. Ali, A. Samanta, Development and evaluation of intestinal targeted mucoadhesive microspheres of *Bacillus coagulans*, Drug Dev. Ind. Pharm. 37 (2011) 1329.
[35] N.G. Sahoo, M. Kakran, L.A. Shaal, L. Li, R.H. Muller, M. Pal, L.P. Tan, Preparation and characterization of quercetin nanocrystals, J. Pharm. Sci. 100 (2011) 2379.
[36] Y. Zhang, M. Huo, J. Zhou, A. Zou, W. Li, C. Yao, S. Xie, DDSolver: an add-in program for modeling and comparison of drug dissolution profiles, AAPS J. 12 (2010) 263.
[37] P. Costa, J.M. Sousa Lobo, Modeling and comparison of dissolution profiles, Eur. J. Pharm. Sci. 13 (2001) 123.
[38] S. Azarmi, H. Valizadeh, M. Barzegar-Jalali, R. Lobenberg, In situ cross-linking of polyanionic polymers to sustain the drug release of Acetazolamide tablets, Pharm. Ind. 65 (2003) 877.
[39] G. Mohammadi, A. Nokhodchi, M. Barzegar-Jalali, F. Lotfipour, K. Adibkia, N. Ehyaei, H. Valizadeh, Physicochemical and anti-bacterial performance characterization of clarithromycin nanoparticles as colloidal drug delivery system, Colloids Surf. B 88 (2011) 39.
[40] M. Jelvehgari, P.Z. Milani, M.R. Siahi-Shadbad, F. Monajjemzadeh, A. Nokhodchi, Z. Azari, H. Valizadeh, In vitro and in vivo evaluation of insulin microspheres containing protease inhibitor, Arzneimittelforschung 61 (2011) 14.
[41] M. Jelvehgari, J. Barar, H. Valizadeh, S. Shadrou, A. Nokhodchi, Formulation, characterization and in vitro evaluation of theophylline-loaded Eudragit RS 100 microspheres prepared by an emulsion-solvent diffusion/evaporation technique, Pharm. Dev. Technol. 16 (2011) 637.
[42] M. Barzegar-Jalali, K. Adibkia, H. Valizadeh, M.R. Shadbad, A. Nokhodchi, Y. Omidi, G. Mohammadi, S.H. Nezhadi, M. Hasan, Kinetic analysis of drug release from nanoparticles, J. Pharm. Pharm. Sci. 11 (2008) 167.
[43] S. Azarmi, J. Farid, A. Nokhodchi, S.M. Bahari-Saravi, H. Valizadeh, Thermal treating as a tool for sustained release of indomethacin from Eudragit RS and RL matrices, Int. J. Pharm. 246 (2002) 171.
[44] Y. Capan, G. Jiang, S. Giovagnoli, K.H. Na, P.P. DeLuca, Preparation and characterization of poly(D,L-lactide-co-glycolide) microspheres for controlled release of human growth hormone, AAPS PharmSciTech 4 (2003) E28.

[45] J.C. Wu, S.G. Su, S.S. Shyu, H. Chen, Effect of the solvent-non-solvent pairs on the surface morphology and release behaviour of ethylcellulose microcapsules prepared by non-solvent-addition phase separation method, J. Microencapsul. 11 (1994) 297.
[46] A.J. Thote, J.T. Chappell Jr., R.B. Gupta, R. Kumar, Reduction in the initial-burst release by surface crosslinking of PLGA microparticles containing hydrophilic or hydrophobic drugs, Drug Dev. Ind. Pharm. 31 (2005) 43.
[47] R. Wickramasinghe, J.L. Liow, Y.K. Leong, Nanobiotech Congress, 2007.
[48] A. Martin, P. Bustamante, A.H. Chun, Physical Pharmacy and Pharmaceutical Sciences, fifth edn, Lippincott Williams & Wilkins, Philadelphia, 2006.
[49] S.M. Agnihotri, P.R. Vavia, Diclofenac-loaded biopolymeric nanosuspensions for ophthalmic application, Nanomedicine 5 (2009) 90.
[50] T. Govender, S. Stolnik, M.C. Garnett, L. Illum, S.S. Davis, PLGA nanoparticles prepared by nanoprecipitation: drug loading and release studies of a water soluble drug, J. Control. Release 57 (1999) 171.
[51] R.K. Averineni, G.V. Shavi, A.K. Gurram, P.B. Deshpande, K. Arumugam, N. Maliyakkal, S.R. Meka, U. Nayanabhirama, PLGA 50:50 nanoparticles of paclitaxel: development, in vitro anti-tumor activity in BT-549 cells and in vivo evaluation, B. Mater. Sci. 35 (2012) 319.
[52] B. Mukherjee, K. Santra, G. Pattnaik, S. Ghosh, Preparation, characterization and in-vitro evaluation of sustained release protein-loaded nanoparticles based on biodegradable polymers, Int. J. Nanomedicine 3 (2008) 487.
[53] S. de Chasteigner, H. Fessi, J.-P. Devissaguet, F. Puisieux, Comparative study of the association of itraconazole with colloidal drug carriers, Drug Dev. Res. 38 (1996) 125.
[54] C. Fonseca, S. Simoes, R. Gaspar, Paclitaxel-loaded PLGA nanoparticles: preparation, physicochemical characterization and in vitro anti-tumoral activity, J. Control. Release 83 (2002) 273.
[55] P. Ahlin, J. Kristl, A. Kristl, F. Vrecer, Investigation of polymeric nanoparticles as carriers of enalaprilat for oral administration, Int. J. Pharm. 239 (2002) 113.
[56] K. Hu, S. Cao, F. Hu, J. Feng, Enhanced oral bioavailability of docetaxel by lecithin nanoparticles: preparation, in vitro, and in vivo evaluation, Int. J. Nanomedicine 7 (2012) 3537.
[57] C. He, L. Yin, C. Tang, C. Yin, Size-dependent absorption mechanism of polymeric nanoparticles for oral delivery of protein drugs, Biomaterials 33 (2012) 8569.